

RESEARCH ARTICLE

Exceptional evolutionary lability of flower-like inflorescences (pseudanthia) in Apiaceae subfamily Apioideae

Jakub Baczyński¹  | Hervé Sauquet^{2,3}  | Krzysztof Spalik¹ 

¹Institute of Evolutionary Biology, Faculty of Biology, University of Warsaw Biological and Chemical Research Centre, Warsaw, Poland

²National Herbarium of New South Wales (NSW), Royal Botanic Gardens and Domain Trust, Sydney, NSW 2000, Australia

³Evolution and Ecology Research Centre, School of Biological, Earth and Environmental Sciences, University of New South Wales, Sydney, Australia

Correspondence

Jakub Baczyński, Institute of Evolutionary Biology, Faculty of Biology, University of Warsaw Biological and Chemical Research Centre, Warsaw, Poland.

Email: jakub.jerzy.baczynski@student.uw.edu.pl

Abstract

Premise: Pseudanthia are widespread and have long been postulated to be a key innovation responsible for some of the angiosperm radiations. The aim of our study was to analyze macroevolutionary patterns of these flower-like inflorescences and their potential correlation with diversification rates in Apiaceae subfamily Apioideae. In particular, we were interested to investigate evolvability of pseudanthia and evaluate their potential association with changes in the size of floral display.

Methods: The framework for our analyses consisted of a time-calibrated phylogeny of 1734 representatives of Apioideae and a morphological matrix of inflorescence traits encoded for 847 species. Macroevolutionary patterns in pseudanthia were inferred using Markov models of discrete character evolution and stochastic character mapping, and a principal component analysis was used to visualize correlations in inflorescence architecture. The interdependence between net diversification rates and the occurrence of pseudocorollas was analyzed with trait-independent and trait-dependent approaches.

Results: Pseudanthia evolved in 10 major clades of Apioideae with at least 36 independent origins and 46 reversals. The morphospace analysis recovered differences in color and compactness between floral and hyperfloral pseudanthia. A correlation between pseudocorollas and size of inflorescence was also strongly supported. Contrary to our predictions, pseudanthia are not responsible for variation in diversification rates identified in this subfamily.

Conclusions: Our results suggest that pseudocorollas evolve as an answer to the trade-off between enlargement of floral display and costs associated with production of additional flowers. The high evolvability and architectural differences in apioid pseudanthia may be explained on the basis of adaptive wandering and evolutionary developmental biology.

KEYWORDS

adaptive wandering, BAMM, diversification, macroevolution, MEDUSA, MuHiSSE, pseudocorolla, umbel

Pseudanthia are inflorescences that resemble a single flower and usually act as a single pollination unit. Although some are formed only with uniform, undifferentiated flowers (i.e., Mimosoideae), their most widespread and derived types bear pseudocorollas: perianth-like structures composed of modified peripheral florets in floral pseudocorollas or of extrafloral organs such as bracts, leaves, entire shoots or stipular

excrescences in hyperfloral pseudocorollas. Pseudocorollar pseudanthia (hereafter, pseudanthia) arose independently in various lineages of angiosperms, including magnoliids (Tucker, 1981; Todzia, 1988), monocots (Rudall, 2003), and eudicots (Cläßen-Bockhoff, 1990). They are particularly common among campanulid asterids (i.e., Bruniaceae, Caprifoliaceae, Adoxaceae) and sometimes postulated to be a key innovation that

This is an open access article under the terms of the Creative Commons Attribution License, which permits use, distribution and reproduction in any medium, provided the original work is properly cited.

© 2022 The Authors. *American Journal of Botany* published by Wiley Periodicals LLC on behalf of Botanical Society of America.

led to the spectacular radiation of Asteraceae—one of the largest angiosperm families and having more than 20,000 species (Jeffrey, 2009; Panero and Crozier, 2016).

Contrary to other key floral traits involved in pollination biology such as floral symmetry (Reyes et al., 2016), color (Smith and Goldberg, 2015; Koski, 2020; Skeels et al., 2021), presence of nectar spurs (Fernández-Mazuecos et al., 2019), or variation in sexual systems (Goldberg et al., 2017), the evolutionary patterns of flower-like inflorescences and their potential link with diversification has not yet been addressed using phylogenetic comparative methods. Our knowledge about ecological importance of pseudanthia is also impaired due to their frequent association with highly generalized pollination systems, which are notoriously difficult to study. Few surveys indicated that perianth-like organs give a strong selective advantage (Sun et al., 2008) and increase seed set (Stuessy et al., 1986), but the fitness gains resulting from such architecture may be dependent on the overall size of inflorescence (Andersson, 1996) and available pollinators niches

(Andersson, 1999, 2008; Celedón-Neghme et al., 2007; Nielsen et al., 2002).

Apioid umbellifers (Apiaceae subfamily Apioideae) with ca. 400 genera and 3000 species constitute the core clade of the campanulid order Apiales and include economically important crops (carrot, parsley) and spices (cumin, coriander, caraway). Their flowers are usually organized into a distinctive, modular inflorescence (Figure 1A), known as compound umbel (umbel composed of umbellets). Its ostensible uniformity in fact hides large variation in spatial and temporal organization, size gradient, and floral sex distribution (Reuther and Claßen-Bockhoff, 2010). Apioids are also the only group of angiosperms where pseudanthia with both floral (Figure 1B) and hyperfloral (Figure 1C) pseudocorollas can be found in closely related plants (Claßen-Bockhoff, 1990). These two types of perianth-like organs occur in combination with differences in shape (flat-surfaced vs. spherical), color (white, yellow, or purple), and size of floral display. The array of different forms of flower-like inflorescences make

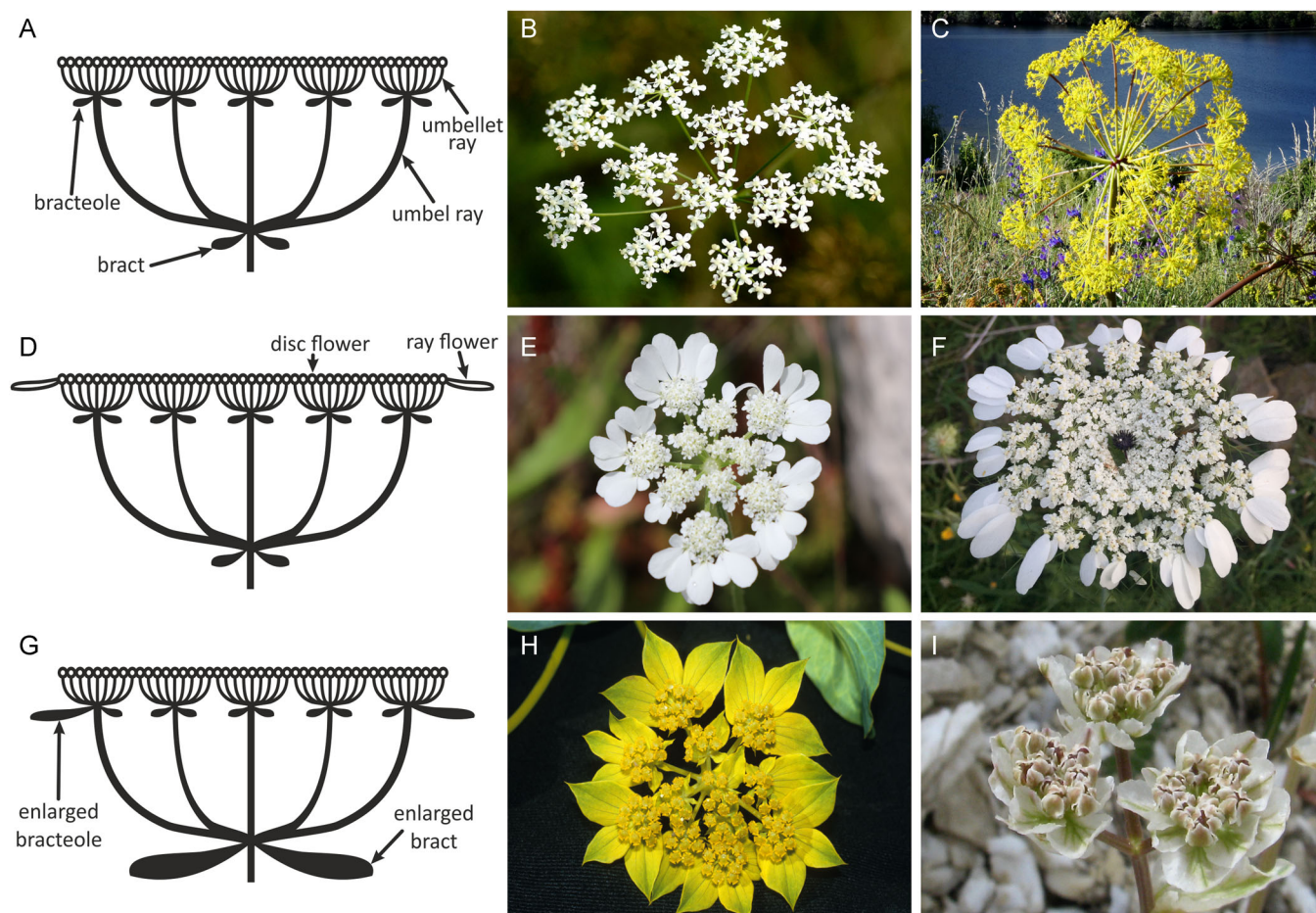


FIGURE 1 Diversity of inflorescences in Apiaceae subfamily Apioideae. (A–C) Compound umbel without a pseudocorolla: (B) *Pimpinella saxifraga* L. and (C) *Ferula communis* L. (D–F) Pseudanthium with a pseudocorolla formed by enlarged peripheral florets: (E) *Tordylium brachytaenium* Boiss. & Heldr. and (F) *Artedia squamata* L. (G–I) Pseudanthium with a hyperfloral pseudocorolla formed by involucellar and/or involucral bracts: (H) *Bupleurum* sp. L. and (I) *Hymenidium nanum* (Rupr.) Pimenov & Kljuykov. Photo credits: (E, F) Jakub Baczyński, Regine Claßen-Bockhoff (H) or adapted from Wikimedia Commons after Udo Schmidt (B), Miguel Angel Masegosa Martínez (C), and Alexey Yakovlev (I)

Apiioideae an interesting model for investigation of their evolutionary significance.

The exact number and phylogenetic placement of independent origins of pseudanthia in Apiioideae has not been reconstructed so far. Fortunately, in the last 20 years much effort has been made to establish a well-supported phylogeny for this subfamily (Downie et al., 1996, 2010; Downie and Katz-Downie, 1996; Katz-Downie et al., 1999; Ajani et al., 2008; Zhou et al., 2008; Magee et al., 2010; Banasiak et al., 2013; Wen et al., 2020; Clarkson et al., 2021) that can be used as a framework for such inference. Apiioideae are also an interesting target for investigation of diversification patterns associated with pseudanthia because the distribution of species within this group is highly uneven among the major clades—often formally recognized as tribes—with some small (e.g., Coriandreae) or monospecific (e.g., Erigenieae) and others (particularly, Selineae and Scandiceae) comprising a few hundred species each (Plunkett et al., 2018). This variation, coupled with a comprehensively sampled molecular phylogeny and multiple independent origins of pseudanthia allow to address the limitations of existing trait-dependent diversification models (Maddison and FitzJohn, 2015; Gamisch, 2016; Rabosky and Goldberg, 2015; May and Moore, 2016; Kodandaramaiah and Murali, 2018; Simpson et al., 2018).

In this study, we investigated evolutionary patterns of pseudanthia using Apiaceae subfamily Apiioideae as a model. By applying a robust macroevolutionary toolkit (ancestral state reconstruction under Markov models and stochastic mapping, morphospace analysis, trait-dependent and trait-independent diversification models) over the most species-rich apioid phylogeny and the largest morphological matrix of inflorescence-derived traits encoded for this group, we aimed to answer the following questions: (1) What are the macroevolutionary dynamics of pseudanthia? (2) Is the evolution of pseudanthia correlated with changes in size of floral display? (3) Are there any morphological correlations in different pseudanthial architectures? (4) What are the diversification patterns of Apiioideae and can they be explained by the evolution of pseudocorollas?

MATERIALS AND METHODS

Taxon sampling and molecular data set

Sequences of nuclear nrDNA ITS and ETS and plastid *rpoCl*, *rps16*, and *rpl16* introns for the species representing Apiaceae subfamily Apiioideae were downloaded from NCBI using MatPhylobi, a bioinformatic tool created by Hanna Kranas and Łukasz Banasiak (<https://github.com/hansiu/MatPhylobi>). The software automatically joins conspecific ITS1 and ITS2 sequences that were frequently obtained and published separately because of historical limitations of sequencing methods. It also allows for specification of a blacklist including accessions previously identified as erroneous or dubious (e.g., obtained from misidentified

specimens or resulting from laboratory contamination with other taxa) by various researchers. The tree was rooted with *Sanicula epipactis* E.H.L. Krause, a representative of subfamily Saniculoideae that constitutes the sister group of apioids (Valiejo-Roman et al., 2002; Calviño and Downie, 2007; Calviño et al., 2008; Clarkson et al., 2021).

We filtered the molecular data set retaining only those species for which the ITS sequence was available. If the sequence was partial (e.g., contained only ITS1 or ITS2), we included the taxon only if at least one plastid marker was additionally sampled. Resulting matrices were aligned separately using the G-INS-I algorithm implemented in MAFFT v.7.271 (Kato and Standley, 2013) and automatically trimmed with trimAl v.1.2rev59 (Capella-Gutiérrez et al., 2009) with the -automated1 option. The resulting matrix comprised 4059 nucleotide positions and 1734 species including representatives of all major lineages (tribes) of Apiioideae. The coverage of markers was 100% for nrDNA ITS, 19% for nrDNA ETS, 15% for both *rpoCl* and *rpl16* introns, and 46% for *rps16* intron. The inclusion of incompletely sampled markers in molecular data sets has proven to be beneficial by rescuing analyses from long-branch attraction and improving phylogenetic resolution (Wiens, 2003, 2005; Wiens and Tiu, 2012; Jiang et al., 2014). Although some authors suggested that missing data can influence branch length estimates (Lemmon et al., 2009; Brown et al., 2010), the bias introduced even with highly incomplete molecular matrices was proven insignificant when available sites retain consistent information about branch lengths (Wiens and Morrill, 2011; Roure et al., 2013; Jiang et al., 2014).

The list of accessions is given in Appendix S1.

Morphological data set

A data set of five quantitative (continuous) and six qualitative (discrete) floral and inflorescence traits was compiled for 847 species of apioid umbellifers (Table 1). The choice of species was primarily guided by the availability of molecular data and designed to account for both phylogenetic and morphological diversity of Apiioideae. Character typology and scoring were mostly based on floristic and taxonomic accounts that, if possible, were verified with online photographs of herbarium specimens and personal observations (the list of main sources used for each species is available in Appendix S2). Because morphological descriptions are inevitably biased by individual perception of (frequently continuous) morphological variation, we applied a strict coding regimen for creating our typology. For example, flowers were scored as “white” only when described as such without any adjectives indicating hues; the latter were assigned to respective states: “yellow/yellowish” (e.g., “yellowish white”, “green-yellow”, “creamy”) or “purple/purplish” (e.g., “purplish tinged”, “purplish white”). The discretization of other traits—sepals and involucre and involucellar bracts—was consistent

TABLE 1 Morphological characters used to score inflorescence traits

Trait name	Coding scheme
Minimum number of umbellets	Primary continuous
Maximum number of umbellets	Primary continuous
Minimum number of flowers per umbellet	Primary continuous
Maximum number of flowers per umbellet	Primary continuous
Average umbel size	Secondary continuous
Outer and inner rays	0, unequal; 1, subequal to equal
Flower color	0, white; 1, yellowish to yellow; 2, purplish to purple
Involucral bracts	0, absent; 1, single; 2, numerous; 3, showy (hyperfloral pseudocorolla)
Involucellar bracts	0, absent; 1, single; 2, numerous; 3, showy (hyperfloral pseudocorolla)
Sepals	0, absent; 1, minute; 2, conspicuous; 3, asymmetric
Ray flowers	0, absent; 1, present (floral pseudocorolla)

TABLE 2 MuHiSSE models fitted for different types of pseudocorollas in trait-dependent diversification analyses. Abbreviations “Div. pars” and “Trans. pars” denote the numbers of diversification rate parameters and transition rate parameters, respectively. The best-fitting model as chosen by AIC_c is marked in boldface. See Appendix S4 for graphical illustrations of different models used in this analysis

Model	Hidden traits	ln L	Div. pars	Trans. pars	AIC _c
MuSSE equivalent (constrained ϵ)	0	-3159.9	4	4	6335.9
MuSSE equivalent	0	-3156.5	6	4	7704.4
MuCID-3 (constrained ϵ)	2	-2649.8	4	18	5344.8
MuCID-3	2	-2628.1	6	18	5305.7
MuHiSSE absent (constrained ϵ)	1	-2669.5	5	6	5361.2
MuHiSSE absent	1	-2667.4	8	6	5363.3
MuHiSSE floral (constrained ϵ)	1	-2682.4	5	6	5387.2
MuHiSSE floral	1	-2707.4	8	6	5443.3
MuHiSSE hyperfloral (constrained ϵ)	1	-2670.0	5	6	5421.9
MuHiSSE hyperfloral	1	-2689.8	8	6	5407.5
MuHiSSE all states (constrained ϵ)	1	-2647.8	7	10	5330.3
MuHiSSE all states	1	-2660.5	12	10	5366.2

across various sources, and we applied it without further adjustments. Although frequently provided in descriptions, the degree of ray flowers' pronouncement (e.g., “outer petals weakly/strongly radiant”) is highly subjective, especially when intraspecific variation is taken into account (Sheppard, 1991). Therefore, in our analyses, we scored only the presence of floral pseudocorollas but not their size.

The scoring scheme allowed for missing data (when the description was incomplete or imprecise) and polymorphisms (indicating variable state of a character in a single species). Average umbel size, a secondary continuous character used in some analyses, was calculated as [(Minimum number of umbellets \times Minimum number of

flowers) + (Maximum number of umbellets \times Maximum number of flowers)]/2. This approach should give a good approximation of inflorescence size for apioids, as their flowers are relatively uniform in size. (Although precise measurements are hardly available, individual florets rarely exceed 4 millimeters in diameter, e.g., Chen and Wang, 2001; Van Wyk et al., 2010; Thakur et al., 2020).

Although this typology may easily be applied to the vast majority of apioids, the taxa with strongly reduced compound umbels such as *Lilaeopsis* (Affolter, 1985) pose a challenge to the formulation of primary homology statements. In this study, we assumed that a derived simple umbel is an equivalent of a single ray from the compound

umbel and its subtending organs are involuellar rather than involuclral bracts.

Phylogeny reconstruction and dating

Phylogenetic inference was conducted with a maximum likelihood (ML) approach implemented in RAxML 8.2.4 with a GTR + G substitution model recommended by the author of the software (Stamatakis, 2014). The data set was divided into two partitions (nuclear and plastid markers) following the results of PartitionFinder 2.1.1 (Lanfear et al., 2012) analyses with the options branch lengths linked and AIC_c. Branch support was evaluated with 1000 rapid bootstrap replicates. Shimodaira–Hasegawa-like approximate-likelihood ratio test (SH-like aLRT) analysis was performed to obtain an alternative measure of branch support, as pseudoreplication-based methods may fail to recover particular nodes when data sets are highly incomplete. Prior to all subsequent analyses, the outgroup was removed from the tree.

The macrofossil record of Apioideae is extremely sparse (Manchester et al., 2015), while palynomorphs used to calibrate previous molecular dating studies were usually assigned to particular nodes at face value (Banasiak et al., 2013; Nicolas and Plunkett, 2014; Wen et al., 2020). More detailed analyses of pollen grains of Apiales (Baczyński et al., 2021) allowed for a choice of more reliable calibration points consisting of four minimum age constraints on internal nodes. Detailed data for the age and node assignment of the fossils are provided in Appendix S3, following the format used by Ramírez-Barahona et al. (2020) to justify angiosperm fossil calibrations. Divergence times were estimated using penalized likelihood (Sanderson, 2002) as implemented in TreePL (Smith and O'Meara, 2012) with the root (crown node) of Apioideae constrained between 42 and 72 Ma in accordance to results of Nicolas and Plunkett (2014) and Wen et al. (2020). The priming analysis and the optimization of smoothing factor were performed before running the final analysis resulting in the following set of parameters: opt = 4, moredetail, optad = 4, moredetailad, optcvad = 4, smooth = 0.1. We refrained from using Bayesian Markov chain Monte Carlo (MCMC) dating because of the limitations on the computational power required to reach convergence due to the large number of taxa included in our data set.

Ancestral state reconstruction and correlation analyses

We reconstructed ancestral states using Markov models and a maximum likelihood (ML) approach as implemented in the corHMM 2.4 package in R (Boyko and Beaulieu, 2020). The analyses were performed separately for the type of pseudocorolla and the average inflorescence size, then on

both traits combined to test for correlated evolution between these two characters. For each analysis, the chronogram obtained with TreePL was pruned to match the morphological data set: 847 taxa for pseudocorollas and 525 taxa for inflorescence size and the two traits combined. Types of pseudocorollas were encoded as a three-state character (0, absent; 1, floral; 2, hyperfloral). As the analyses required qualitative data, inflorescence size was discretized based on tertiles of its distribution resulting in three states: small (<82 flowers), medium (83–214 flowers), and large (>214 flowers). To compute the total number of state changes for the type of pseudocorolla, we used a stochastic mapping approach with the makeSimmap function (500 simulations across the tree) implemented in corHMM package. To account for potential impact of different coding scheme for recovered instances of pseudanthia origins, the analysis was replicated by combining floral and hyperfloral pseudocorollas as a single state (0, absent; 1, present; see Appendix S4).

To check the assumptions on directions of evolutionary transitions in inflorescence size and type of pseudocorolla, we compared ordered and unordered versions of all models for both these traits (Appendix S5A). Our preliminary analyses indicated that different types of pseudocorollas cannot directly evolve one into another but have to pass through the state “absent”, suggesting that this trait is ordered. Inflorescence size was also reconstructed as an ordered character with transitions between small and large umbels occurring via the “medium” state.

We further analyzed the type of pseudocorollas and inflorescence size jointly to test for correlated evolution between these two characters. We applied maximum likelihood tests derived from Pagel's (1994) method. The combination of our two three-state characters resulted in a transition rate matrix of nine by nine possible state combinations, with 72 transition rate parameters. However, ordering both characters allowed for matrix to be reduced to 24 parameters in the most complex model. By editing the combination of ordered transition matrices for both traits, we fitted two variants of SYM and ARD models for the combination of the two traits: correlated (the state of one character affects the relative transition rates of a second) and uncorrelated (states of characters change independently from each other). The schematic diagrams of all transition matrices are listed in Appendix S5A.

Principal component analysis

A principal component analysis was performed to investigate correlations in inflorescence architecture, which could have evolved in response to certain selective drives (e.g., adaptive wandering). Specifically, we used a mixed PCA approach implemented in R package PCAmixdata 3.1 (Chavent et al., 2014). This method handles a combination of both qualitative and quantitative data using generalized singular value decomposition but, unfortunately, does not

allow for phylogenetic correction (Nye, 2011; Polly et al., 2013). The coding scheme followed Table 1, resulting in 23 distinct eigenvectors corresponding to either state (for qualitative data) or trait (for primary quantitative data). As no form of multidimensional scaling can tackle polymorphic qualitative characters, we decided to use the approach presented in Chartier et al. (2017). Briefly, this approach involved repeated random solving of polymorphisms (choosing one for each case) and re-running the analysis to ascertain that initial differences do not affect data visualization. Additionally, to ensure that our data set has a structure that creates at least one distinct eigenvalue, we compared values of ψ and φ statistics on 100 replicates of unrandomized and randomized matrices (values for each trait are shuffled independently), following Björklund (2019). The scree plots for eigenvalues were inspected for both variants to determine how many principal components to interpret. The results were visualized with ggplot2 3.3.2 (Wickham, 2016).

To explore the influence of different ordination techniques on the reconstruction of morphospace, we applied NMDS (nonmetric multidimensional scaling) based on Gower distances (Appendix S6A), as implemented in the R package *vegan* 2.5-6 (Oksanen et al., 2013). The polymorphisms were solved 100 times, according to the method described above. The homogeneity of dispersion for different pseudanthial architectures (absent, floral and hyperfloral) was tested using the *betadisper* function (Appendix S6B), which performs a multivariate analogue of Levene's test for homogeneity of variances. To check for significant differences of the groups' centroid/dispersion, we performed the permutational multivariate analysis of variance (PERMANOVA), available under the *adonis* function.

Trait-independent diversification analyses

Trait-independent diversification rate shift analyses were performed on the TreePL chronogram with a stepwise AIC-based approach as implemented in MEDUSA (Alfaro et al., 2009) and with Bayesian analysis of macroevolutionary mixtures (BAMM: Rabosky et al., 2014). Despite concerns surrounding both methods (May and Moore, 2016; Moore et al., 2016; Rabosky et al., 2017; Rabosky, 2018) and the use of dated molecular phylogenies to estimate parameters of generalized birth–death models in general (Louca and Pennell, 2020), we believe that this type of inference will at least allow us to test for net diversification rates heterogeneity within Apioideae. MEDUSA analyses were conducted in R with package *geiger* 2.07 using three available methods: pure Yule, birth–death, and a mix of these processes. BAMM was run over 100 million generations with initial parameters estimated with R package *BAMMtools* 2.1.7. The analysis was repeated with three different Poisson rate priors (0.05, 0.1, 0.2) and expected number of shifts (5, 10, 20) to ensure that the results are not

entirely conditioned by these settings (Moore et al., 2016). Each variant reached convergence with estimated samples sizes >200 after initial 10% burn-in. Because MEDUSA and BAMM both assume complete sampling within analyzed clades, we provided the information about species richness by evenly distributing missing species among sampled representatives of each genus (Appendix S7A, B). The information about generic level diversity of apioids (Appendix S7D) was taken from Plants of the World Online (<http://www.plantsoftheworldonline.org/>) and—whenever necessary—corrected following the most recent taxonomic revisions (Spalik et al., 2004; Sun et al., 2004; Ronse et al., 2010; Banasiak et al., 2016). To investigate how this approach may influence the estimates of diversification rates, we also replicated the BAMM and MEDUSA analyses without specifying the sampling fraction.

Trait-dependent diversification analyses

To address the influence of different types of pseudanthial pseudocorollas on diversification rates within Apioideae, we used one of the most recent members of the ever-expanding family of state speciation and extinction (SSE) models. MuHiSSE (Nakov et al., 2019), implemented in the R package *hisse* 1.9.10, applies the framework developed within HiSSE (Beaulieu and O'Meara, 2016; Caetano et al., 2018) to MuSSE (Multiple State Speciation and Extinction; FitzJohn, 2012) to account for the potential impact of additional factors or traits on rate heterogeneity within the tree and to deal with multiple state/traits at the same time. While earlier iterations of SSE models independently estimate speciation (λ), extinction (μ), and transition rate parameters (q), MuHiSSE fits derived measures of diversification defined as turnover ($\tau = \lambda + \mu$; rate of birth or death per unit of time) and extinction fraction ($\varepsilon = \mu/\lambda$; ratio of death and birth events per unit of time).

Using maximum likelihood, we fitted a set of 12 MuHiSSE models with increasing complexity (Table 3, Appendix S5B) to a data set comprising the morphological matrix with 847 taxa and the chronogram pruned to match it. Similar to the ancestral state reconstruction analyses, pseudocorollas were treated as an ordered character. To take incomplete taxonomic sampling into account, we specified the sampling fraction for each of the three states (probability of an extant species in a particular state being included in the phylogeny). While assessing these parameters, we used an indirect approach because the descriptions of many species were not easily available or lacked information on inflorescence architecture. First, for each sampled polymorphic genus (with more than one character-state present among its representatives), we calculated the proportions of species with particular character states using the available data and assumed that these proportions applied to the entire genus. The number of species in each genus was taken from the Plants of the World Online

TABLE 3 CorHMM models fitted for different types of pseudanthial pseudocorollas, size and both traits combined. The best models, chosen with AIC_c , are marked in boldface

Trait	Rate parameters	ln L	No. of parameters	AIC_c
Pseudocorollas	Ordered ER	-332.7	1	667.5
Pseudocorollas	Ordered SYM	-332.7	2	669.4
Pseudocorollas	Ordered ARD	-287.3	4	582.7
Pseudocorollas	ER	-337.1	1	676.2
Pseudocorollas	SYM	-332.7	3	671.4
Pseudocorollas	ARD	-287.3	6	586.8
Size	Ordered ER	-549.2	1	1100.4
Size	Ordered SYM	-545.6	2	1097.2
Size	Ordered ARD	-542.8	4	1093.6
Size	ER	-575.2	1	1152.5
Size	SYM	-545.6	3	1097.2
Size	ARD	-542.8	6	1097.7
Pseudocorollas + size	Ordered SYM, uncorrelated	-771.3	4	1575.6
Pseudocorollas + size	Ordered ARD, uncorrelated	-742.4	8	1537.5
Pseudocorollas + size	Ordered SYM, correlated	-758.8	12	1595.1
Pseudocorollas + size	Ordered ARD, correlated	-726.3	24	1530.0

(POWO) database. For example, *Chaerophyllum* is represented by 33 species in our data set, but 70 species in total are currently accepted. Of the species sampled in our data set, three (9.1%) have floral pseudocorollas, seven (21.2%) have hyperfloral pseudocorollas, while in 23 species (69.7%), pseudocorollas are absent. In polyphyletic genera (such as *Heracleum*), unsampled species were presumed to be distributed evenly among different clades. The genera that were monomorphic based on sampled species were also assumed to be monomorphic across all species.

All models were tested in two variants—with a single extinction fraction (ϵ) across all states or with varying extinction fraction—and subsequently evaluated using AIC_c . First, we fitted MuSSE-like models (without hidden traits) assuming that changes in diversification rates are driven only by the observed character. MuHiSSE (with hidden traits) models were then optimized with hidden state associated only with one of the observed states, i.e., separately for the absence of pseudocorollas, for floral pseudocorollas, and for hyperfloral pseudocorollas, and then with all these three states at once. MuCID (multistate character-independent) models with diversification parameters unlinked to observed traits were used as a null hypothesis. Specifically, we optimized MuCID-3, a “fair competitor” for MuSSE models sharing the same number of diversification parameters (Beaulieu and O’Meara, 2016). Graphs visualizing all used rate matrices are given in Appendix S5B.

Furthermore, we tested for trait-dependent diversification with floral and hyperfloral pseudanthia treated as a single state to elucidate the effect of sheer pseudocorolla presence (without distinguishing between its different types) on speciation and extinction rates. The fitted models were equivalent to those used in the multistate approach, although redesigned to account for a binary character (BiSSE-like, CID-2, CID-4, and HiSSE).

RESULTS

Phylogeny and divergence times

The results of our phylogenetic analyses (Appendix S8) are consistent with published studies (Ajani et al., 2008; Zhou et al., 2008; Downie et al., 2010; Banasiak et al., 2013), including recent phylotranscriptomic analyses of Apioideae or Apiales as a whole (Wen et al., 2020; Clarkson et al., 2021). Our reconstructed topology indicates that Choritenieae +Lichtensteinieae constitute the sister group to the rest of the subfamily, followed by other African apioids (Annesorhizeae, Heteromorpheae, and Chamaesieae), early-diverging apioids (Bupleureae, Pleurospermeae, Komarovieae, Oenantheae) and two large sister clades of core Apioideae—‘Scandiceae and relatives’ and the apioid superclade. The backbone relationships and almost all tribes/groups were highly supported by bootstrap (>70%) and/or SH-like aLRT (>95%). The results of our divergence time

analysis show that all major lineages originated and diversified about 10 Mya earlier than the estimates of Banasiak et al. (2013) and Wen et al. (2020). As this study was not designed to directly address the phylogeny or timing of major divergence events in Apioideae, these results will not be further discussed here.

Ancestral state reconstruction

The evolution of pseudocorollas is best explained by the ordered ARD model ($\Delta\text{AIC}_c < 2$; Table 3; Appendix S5A) with rates of gains being more than one order of magnitude lower (0.003 and 0.004 for floral and hyperfloral pseudocorollas, respectively) than reversals (0.040 and 0.010, respectively). Unordered versions of investigated models estimated the rate of direct changes between floral and hyperfloral pseudocorollas as zero, effectively reconstructing identical patterns to their ordered equivalent. Pseudanthia were ancestrally absent in Apioideae and results of stochastic mapping (Figure 2) recovered between 93 and 144 state changes for this character (with 95% CI for number of transitions being 115–117). Floral pseudocorollas were acquired less frequently (95% CI of 19–20) than hyperfloral ones (28–29) with a very similar number of losses recorded for both these architectures (32–33 vs. 34–35 reversals on average). The lowest numbers of origins and losses of pseudanthia were reconstructed as 36 and 64, respectively. When treated as a single character (Appendix S4D), pseudocorollas were estimated to have originated between 34 and 66 (95% CI of 52–54) with 40 to 113 subsequent losses (95% CI of 62–65). In this scenario, the ARD model was also chosen as the best fit.

Hyperfloral pseudocorollas are common in early-branching apioids and evolved in Komarovieae, Bupleureae, the *Pleurospermopsis* clade, and Pleurospermeae. In later-diverging apioids, this architecture is rare and dispersed among several distantly related genera: *Chaerophyllum* (Scandiceae), *Hyalolaena* (Pyramidoptereae), *Vesper* (Selineae), and a part of the polyphyletic genus *Hymenidium* (Figure 2; Appendices S4D, S5C). In contrast, floral pseudocorollas appeared relatively late in Apioideae and evolved independently in Oenanthae and Scandiceae and at the base of a large clade composed of Echinophoreae, the *Sinodielsia* clade, the *Cachrys* clade, Tordylieae, Coriandreae, and Selineae.

In contrast to pseudocorollas, the ancestral state for average inflorescence size was ambiguous not only at the root, but also along the backbone of apioid phylogeny (with all three size classes being almost equally likely; Appendix S5D). Large umbels are rather uncommon in early-diverging apioids, appearing more frequently in Scandiceae and relatives (mostly in Ferulinae and Daucinae) and the apioid superclade (especially, Selineae and Tordylieae). The best-fitting model was the ordered ARD model ($\Delta\text{AIC}_c < 2$, Table 3) with transition rates from small to medium (0.21), and medium to large inflorescences (0.010) being higher

than changes in the opposite direction (respectively 0.16 and 0.078). As for the pseudocorolla character, unordered versions of models of inflorescence size evolution suggested that direct transitions between small and large inflorescences are unlikely, with the estimated rates close to zero. This result supports the notion that umbel size in Apioideae changes gradually rather than abruptly in the course of evolution.

The analysis of combined umbel size and pseudocorolla type (Figure 3) strongly indicated that the evolution of these traits is correlated and best explained by an ARD model ($\Delta\text{AIC}_c < 2$, Table 3). The most likely ancestral state for Apioideae was reconstructed as large, non-pseudanthial inflorescence. While hyperfloral pseudocorollas may originate in either small or large umbels, floral ones appear only in the latter. In all aforementioned evolutionary scenarios, the losses are favored over gains, especially for hyperfloral pseudocorollas (0.25 over 0.017 for small and 0.016 over 0.0029 for large inflorescences). The transition rates from medium-sized inflorescences to pseudanthia (floral and hyperfloral) are estimated as zero, and a similar pattern was found for transitions between small-sized inflorescences and floral pseudanthia (in both directions). The increase of inflorescence size is more common than the decrease in non-pseudanthial lineages, whereas in pseudanthial lineages the trend is reversed.

Principal component analyses

In the principal component analyses, the ψ and ϕ statistics for randomized data sets were lower than unrandomized ones across all replicates indicating that the original data set has a biologically meaningful structure. The first two principal components (PCs) explain 24% of the variance within the data set (Figure 4); therefore, we also checked the combinations of the first five PCs that together accounted for over 50% of the variance (Appendix S9). All analyzed PCs were situated above the elbow of scree plot and had higher eigenvalues than their randomized equivalents.

In the morphospace defined by first two PCs, species with floral pseudocorollas do not overlap with those having hyperfloral pseudocorollas; however, both groups partly overlap with those without pseudocorollas (Figure 4). The presence of ray flowers is correlated with asymmetric sepals and, to a lesser extent, unequal outer and inner rays (i.e., outer rays longer than inner ones resulting in a flat inflorescence surface), white petals, and the presence of involucre and involucre bracts. Hyperfloral pseudocorollas are not strongly linked to any characters analyzed although species with this trait generally occupy a part of the morphospace defined by yellow petals and subequal/equal outer and inner umbel rays. Parameters describing inflorescence size (the numbers of umbel rays and of flowers) very weakly contribute to the first five principal components and are unable to explain differences between the floral and hyperfloral pseudanthia.

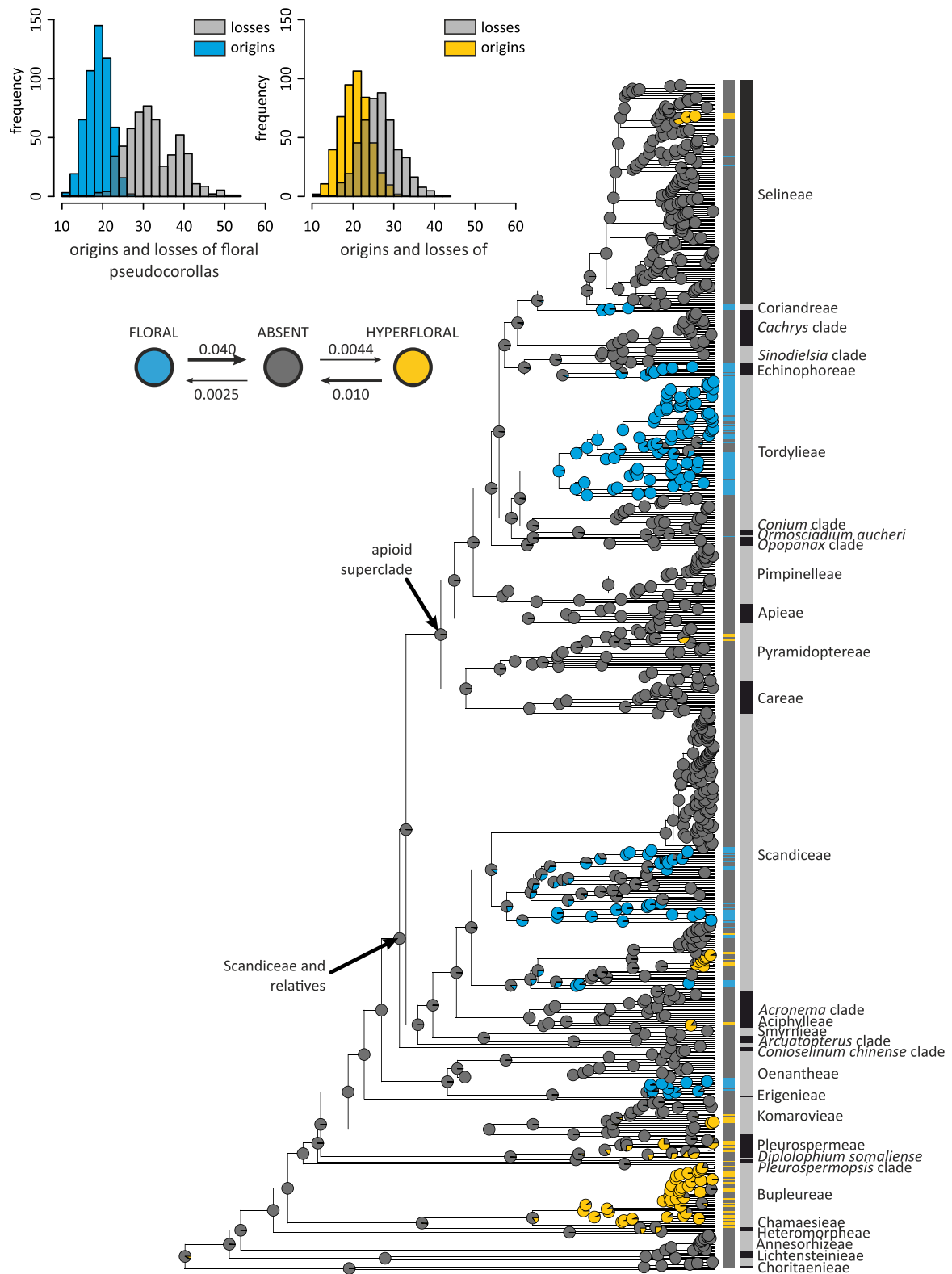


FIGURE 2 SIMMAP reconstruction for pseudocorolla type in Apiaceae subfamily Apioideae averaged across 500 stochastic character-mapped trees. Pie charts at each node represent the probabilities for each state (gray: absent, blue: floral pseudocorollas, yellow: hyperfloral pseudocorollas). Boxes on the right side of the tree indicate tip states. Histograms represent the inferred number of origins and reversals for floral and hyperfloral pseudocorollas. The plot below the histograms shows a visualization of the transition rate matrix resolved by corHMM, with arrow widths proportional to transition rates

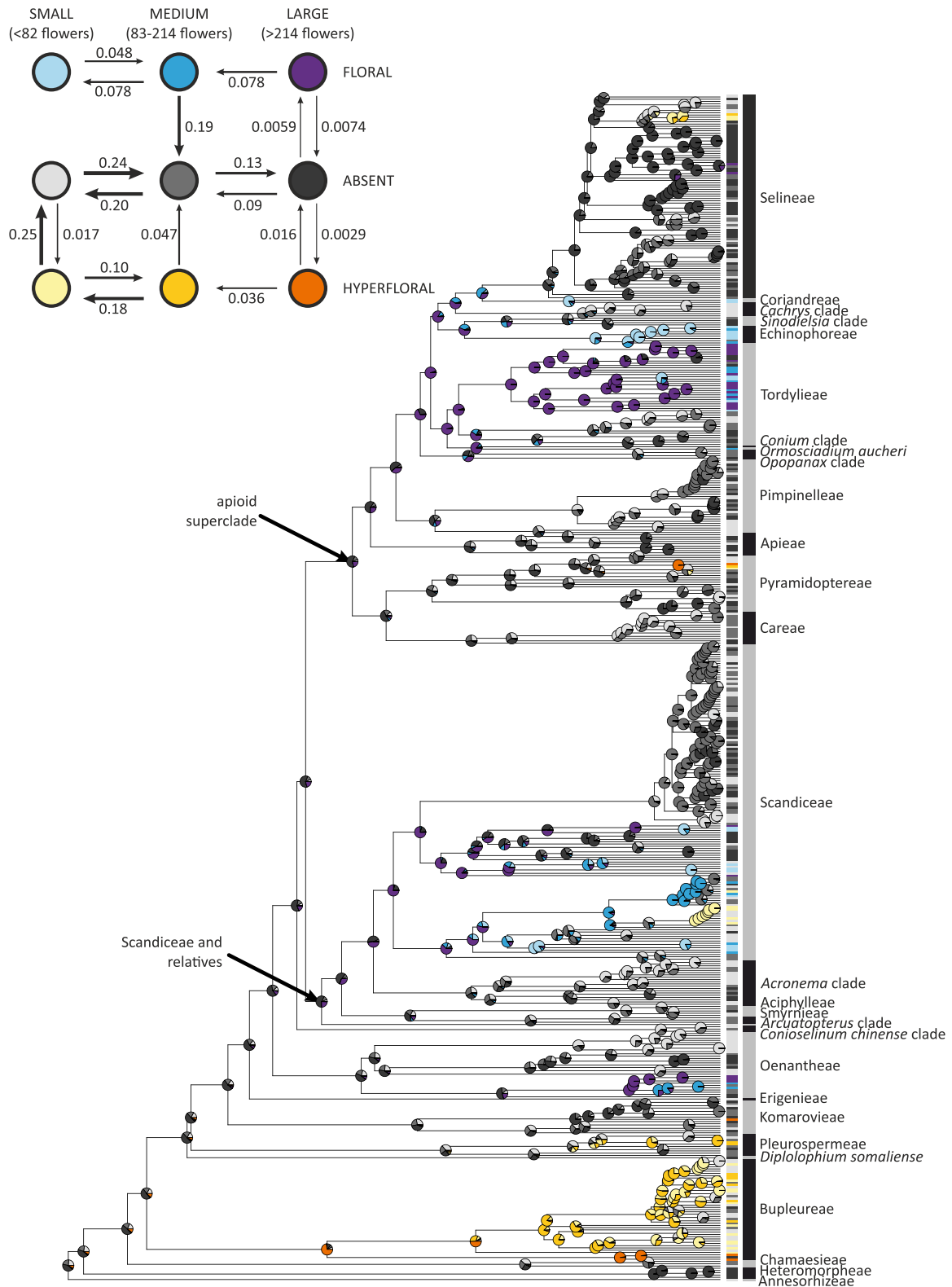


FIGURE 3 Maximum likelihood reconstruction of ancestral states for the correlated model of combined inflorescence size and type of pseudocorolla. The plot in the top-left corner shows a visualization of the transition rate matrix with arrow widths proportional to transition rates. Transitions rates estimated as zero are not shown. Boxes on the right side of the tree indicate tip states. For ancestral state reconstructions of pseudocorollas and inflorescence size treated separately, see Appendix S5C,D

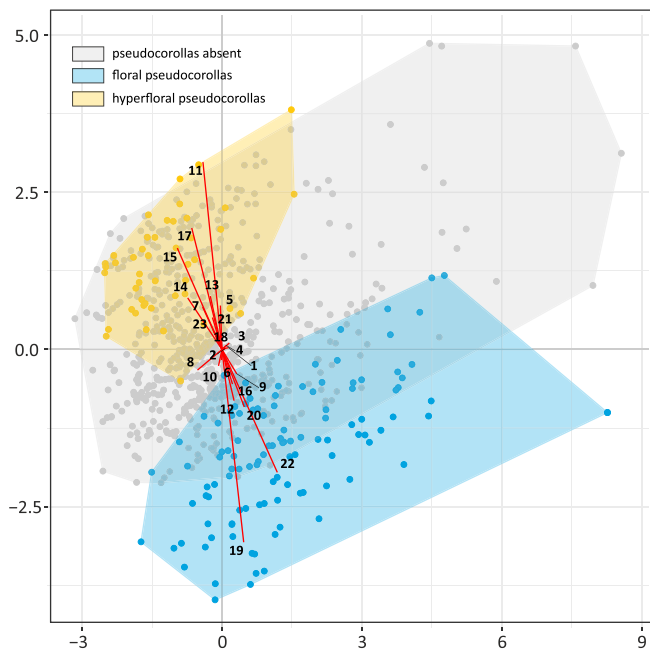


FIGURE 4 Principal component analysis (PCA) for the mix of qualitative and quantitative inflorescence traits. The plot shows the first two principal components, which together explain 24% of the variance. Each point represents a species with colors indicating presence of floral (blue) or hyperfloral (yellow) pseudocorollas. Convex hulls represent parts of the morphospace occupied by species with each of these traits. Numbers at tips of eigenvectors indicate associated trait/state: 1, minimum number of rays; 2, maximum number of rays; 3, minimum number of flowers per umbellet; 4, maximum number of flowers per umbellet; 5, outer and inner rays equal to subequal, 6, outer and inner rays unequal; 7, flowers yellow to yellowish; 8, flowers purple to purplish; 9, flowers white; 10, single involucre bract; 11, involucre bracts showy; 12, involucre bracts numerous; 13, involucre bracts absent; 14, single involucre bract; 15, involucre bracts showy; 16, involucre bracts numerous; 17, involucre bracts absent; 18, sepals minute; 19, sepals asymmetric; 20, sepals conspicuous; 21, sepals absent; 22, ray flowers present; 23, ray flowers absent

The results of betadisper indicate that the variance between groups is heterogeneous across all 100 replicates and thus violates one of the assumptions of PERMANOVA. However, as our design is unbalanced in a way that larger groups have larger dispersion, we expect conservative behavior of PERMANOVA that makes type I error less likely to occur (Anderson and Walsh, 2013). Therefore, we report that the centroid of species with floral pseudocorollas was significantly different from centroids of remaining groups (Appendix S6B). The stress value in each replicate of NMDS analysis was below 0.2, indicating that the produced plot (Appendix S6A) provides good representation of reduced dimensions.

Diversification rate analyses

Character-independent analyses performed with BAMM and MEDUSA point to a high variation in diversification rates within Apioideae, with BAMM reconstructing 26–31 shifts (highest posterior density range) for analyses

with specified species richness and 19–22 shifts when this parameter was not provided (Figure 5; Appendix S10G–X). MEDUSA analyses yielded similar results but with fewer inferred rates (e.g., 21 for the mixed process with species richness correction; Figure 5; Appendix S10A–F). Clades consistently linked with elevated diversification rates across all tested models are tribes Selineae, Aciphylleae, and Bupleureae and genera *Pimpinella* (Pimpinelleae), *Heracleum* (Tordylieae), *Chaerophyllum*, and *Ferula* (both Scandiceae). The *Cachrys* clade, Annesorhizeae, and *Bunium* (Pyramidoptereae) were also frequently associated with such an increase.

The analyses with character-dependent models indicate that the heterogeneity of diversification parameters within Apioideae is independent of the presence or absence of pseudocorollas. The best-fitting model was a MuCID-3 ($\Delta AIC_c < 2$; Table 2), in which diversification rates do not depend on the state of the observed character. The character-independent model (CID-4) was also chosen as the best fit when two types of pseudocorollas were encoded as a single state (Appendix S4C).

DISCUSSION

The presence of pseudanthia is evolutionary labile with 95% confidence interval for total number of transitions reconstructed as 115–117 and at least 36 independent origins in a moderately large clade like Apioideae (Figure 2). Although limited, data available for several lineages of Asteraceae indicate that, in other plant groups, these structures are also prone to convergence (Francisco-Ortega et al., 1999; Sanz et al., 2008; Panero et al., 2014). The high evolvability of flower-like inflorescences can be tentatively explained by the developmental preadaptation and their inability to cause an irreversible phenotypical and ecological specialization, which would hinder eventual losses and re-gains. According to our results, we hypothesize that the main factors responsible for numerous origins of pseudanthia are optimization of floral display size and adaptive wandering within generalized pollination syndromes. Because evolution of pseudocorollas is unlikely to lead to a pollinator-mediated speciation, this trait alone cannot explain diversification patterns in Apioideae and is unlikely to provide such an explanation in other plant groups.

Adaptive wandering of flower-like inflorescences

Generalist pollination systems are frequently considered suboptimal because flowers have to specialize to mitigate trade-offs resulting from mutually exclusive demands and qualitative differences between various pollinators (Ohashi et al., 2021). Some generalist plants, however, could have reached a stable equilibrium (adaptive generalization) with a

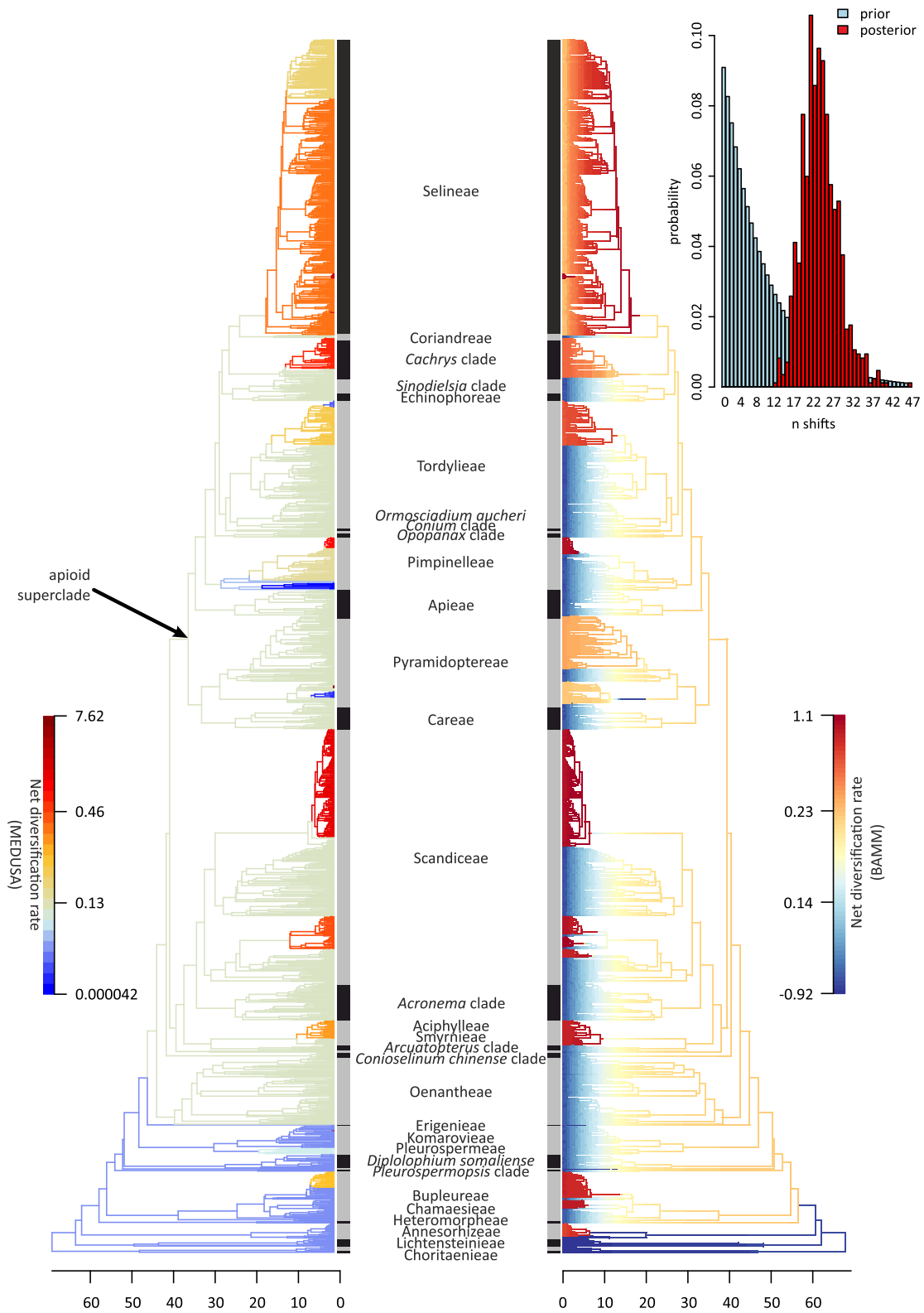


FIGURE 5 Shifts in net diversification rates as estimated with MEDUSA (left) and BMM (right) analyses. The plot in the top-right corner shows prior and posterior probabilities for inferred number of shifts (n) in BMM. Thermal gradient for BMM was scaled with Jenks natural breaks method (nonlinear) because rates across the phylogeny were skewed toward higher values. Due to the large number of investigated models, we show only the results for the “mixed” MEDUSA and BMM analyses with five expected shifts and Poisson rate prior equaling 0.05, both with specified richness. The results of the remaining trait-independent diversification analyses are given in Appendix S10

tight adjustment to available pollinator niches. This mechanism, known as adaptive wandering, is expected to lead to evolution of various phenotypic traits that attract more beneficial pollinators without exclusion of others (Wilson and Thomson, 1996; Dilley et al., 2000; Thomson and Wilson, 2008; Gómez et al., 2014, 2015). Because the nature of such adaptations is described as “transient, reversible and idiosyncratic” (Thomson and Wilson, 2008, p. 25), we may expect them to be highly labile and easily lost during evolution. Umbellifers are generally regarded as ecologically “promiscuous” with a large number of visiting pollinators and frequent spatiotemporal fluctuations in their composition (Lamborn and Ollerton, 2000; Davila and Wardle, 2008). Some researchers speculated that, despite superficial generalism, Apiaceae may undergo “cryptic specialization” with variation of some traits resulting from selection toward specific pollination niches (Bell, 1971; Lindsey and Bell, 1985; Pérez-Bañón et al., 2007; Niemirski and Zych, 2011; Zych et al., 2014, 2019). Pseudocorollas constitute an auxiliary pool of such phenotypic characters that in combination with other traits can be used to reach particular fitness peaks during such adaptive wandering. The high number of transitions (especially reversals) recovered for both types of pseudocorollas (Figure 2) creates a landscape congruent with this evolutionary scenario.

The important question to ask is how specific pseudanthial architectures answer the demands of various pollinators? Our morphospace analysis (Figure 5; Appendices S6, S9) implies existence of disjunct sets of correlated traits in floral and hyperfloral pseudocorollas that in combination with minor phenotypic characters can make displays attractive to particular groups of insects. According to these results, petaloid bracts are strongly associated with yellow or purple flowers and subequal/equal outer and inner umbel rays (making the inflorescence more spherical and less compact). Hyperfloral pseudocorollas found in numerous yellow-flowered representatives of the genus *Bupleurum* are sometimes intensively colored and very prominent (e.g., *Bupleurum aureum* subsp. *porfirii* Kamelin), making them more appealing to visually sensitive pollinators. Such coloration patterns, however, show some degree of polymorphism. For example, *Hymenidium apiolens* Lindley includes three color variants of involucre margins (white, pink, and purple), probably in response to differences in pollination niches (Guo et al., 2020). White petaloid bracts are frequently associated with deeply purple flowers, which may enhance contrast and serve as visual cues for dipterans, especially carrion flies. Hyperfloral pseudocorollas can additionally have deeply colored, reddish veins (e.g., *Pleurospermum amabile* W.G. Craib & W.W. Sm. or *Vesper purpurascens* (A. Gray) R.L. Hartm. & G.L. Nesom.), which further mimic the appearance of flesh.

A distinct morphology and different evolutionary correlations can be found in species with floral pseudocorollas, the blossoms of which are universally white and frequently create a flat surface due to unequal outer and

inner umbel rays. White, inconspicuous flowers are generally considered a mark of generalist pollination systems, but their aggregation in compact, showy pseudanthia may be favored by particular group of insects and beneficial under pollinator limitation. This hypothesis can account for differences between two subspecies of *Heracleum sphondylium* (Zych, 2002, 2007) with apomorphic yellow, loose inflorescences found in *H. sphondylium* subsp. *sibiricum* (L.) Simonk. evolving as a visual cue for lowland beetles, while compact, white-flowered and pseudocorollar umbels of *H. sphondylium* subsp. *sphondylium* (L.) are a plesiomorphic adaptation to flies and wasps in ancestral montane habitats. Moreover, many apioids with white petals and floral pseudocorollas (e.g., *Daucus carota*, *Artemisia squamata*, and some species of *Echinophora* L.) develop so-called “dark central florets”, which have been thought to attract certain species of coleopterans (Westmoreland and Muntan, 1996; Goulson et al., 2009) and flies (Eisikowitch, 1980) or facilitate pollinator’s orientation during foraging (Polte and Reinhold, 2013).

Pseudanthia evolve in response to constraints on floral display size

It is frequently assumed that the number of pollinator visitations and the number of flowers probed per visit are positively correlated with display size, and these interdependences have been proven true both on theoretical grounds (Ohashi and Yahara, 1999) and an experimental basis (Ohara and Higashi, 1994; Grindeland et al., 2005). The attractivity of large inflorescences is particularly clear for dense, multiflowered units like umbels (Ishii et al., 2008), but their augmentation cannot proceed indefinitely without diminishing returns resulting from the risk of geitonogamy (Robertson, 1992; Harder and Barrett, 1995) and production-associated costs (Harder and Johnson, 2005). The risk of geitonogamy (pollination between flowers of the same plant) may be particularly high in flat-surfaced displays as their architecture encourages inconsistent foraging pathways, frequent revisitations, and pollen discounting (Ohashi and Yahara, 2001, 2002; Harder et al., 2004). The opposite size trends (Figure 3) recovered for pseudanthial and non-pseudanthial inflorescences indicate that similar attractiveness can be achieved either by increasing the number of individual flowers or through the formation of pseudocorollas; the latter are likely to evolve in response to constraints on the former.

The modular architecture of apioid pseudanthia allows for their compactness and promotion to be altered as a means of balancing between the attractiveness to pollinators (overall size of floral display) and offspring genetic diversity (related to the number of visits required to pollinate all reproductive units). In large-sized umbels, pseudanthia frequently develop at the level of individual umbellets rather than the entire umbel, forming several distinct, smaller units that cannot be freely explored without considerable

energetic expense (i.e., flight or prolonged walk). This situation is fairly common in tribe Tordylieae, which has a high prevalence of species with floral pseudocorollas (Figure 2). Conversely, in situations of pollinator limitation or when plant population densities are very high, a strong condensation of umbellets within the umbel into a single pseudanthium may be favored as competitively superior (e.g., *Daucus carota* or *Artemisia squamata*).

Massive displays are of great adaptive value under pollinator limitation but require lots of resources and are hardly sustainable. Many umbellifers with such inflorescences (e.g., representatives of *Ferula* L., *Heracleum* or *Angelica*) are monocarpic perennials, which produce spectacular blossoms made of tens of thousands of florets but only once in a lifetime, following several seasons of vegetative growth. In our study, small pseudanthia were reconstructed to evolve predominantly by reduction of larger inflorescences (Figure 3). Because advertising organs demand less resources than flowers (Thomann et al., 2015; Cerca et al., 2019), the development of pseudocorollas may help to diminish the investment in reproductive structures without sacrificing the attractiveness of inflorescence. In this scenario, pseudanthia may first appear as tools for counterbalancing the trade-offs associated with large displays and can later be co-opted in adaptive wandering, particularly to facilitate adaptation to habitats where pollinator limitation is common. This mechanism could potentially explain why among apioids pseudanthia are common in many montane or arid-adapted species, such as representatives of the genera *Tordylium*, *Echinophora*, *Dicyclophora*, or *Pleurospermum*. Interestingly, similar secondarily compartmented or aggregated inflorescences (syncephalia) occurring in Asteraceae subtribe Nassauvinae are also considered an adaptation to dry habitats (Katinas et al., 2008; Katinas and Forte, 2020).

Developmental perspective on the evolutionary lability of pseudanthia

An interesting question concerning pseudanthia in Apioideae is how can such complex structures be so easily “turned on” and “off” in response to selection pressures. The proximal causes underlying this macroevolutionary phenomenon may to some extent be explained on the grounds of evolutionary developmental biology. As the exact molecular mechanisms underlying the formation of different architectures in compound umbels are currently unknown, the inference in this matter must be made based on the data available for distantly related plants. In the case of *Cornus* L. (Zhang et al., 2008; Feng et al., 2012) and *Davidia* Baill. (Vekemans et al., 2012) from the order Cornales, hyperfloral pseudocorollas are patterned by genes otherwise responsible for petal identity (B- and C-class MADS box genes), whose expression shifted to encompass bracts. This shift had been preceded by the duplication of at least some of the aforementioned genes (most

notably, orthologues of *GLOBOSA/PISTILLATA*), allowing paralogues to gain new or additional functions without losing the original one. On the contrary to ray flowers, which are restricted to Apioideae, hyperfloral pseudocorollas are relatively common in all subfamilies of Apiaceae (e.g., *Sanicula epipactis* L. in Saniculoideae, *Pozoa coriacea* Lag. in Azorelloideae, *Actinotus helianthi* Labill. in Mackinlayoideae). As we are not aware of any species with pseudanthia in other families within Apiales (Myodocarpaceae, Araliaceae, Pittosporaceae, Griselinaceae, Torricelliaceae, the expansion of MADS-box genes (or different genetic alteration that accounts for origin of bract petaloidy) must have taken place after the divergence of umbellifers.

The independent gains of floral pseudocorollas across angiosperms are usually associated with *CYCLOIDEA* genes, which expanded their initial role in the establishment of floral symmetry (Fambrini and Pugliesi, 2017) to control the specialization of florets (Tähtiharju et al., 2012; Claßen-Bockhoff et al., 2013; Berger et al., 2016; Zhao et al., 2020). The search for *CYCLOIDEA* genes in the genomic data for carrot (Scandiceae) and coriander (Coriandreae) has so far revealed two paralogues, which must have been present in their last common ancestor (both species develop floral pseudocorollas; J. Baczyński et al., unpublished data). Knowing that some representatives of Oenantheae also develop ray flowers, it is probable that the duplication occurred in the common ancestor of these lineages. The subsequent repeated recruitment/derecruitment of already existing CYC paralogues could be the “molecular switch” responsible for numerous gains and losses of floral pseudocorollas in Apioideae. This explanation is especially tempting in the light of recent studies documenting exceptionally high number of transitions between actinomorphy and zygomorphy (Reyes et al., 2016; Joly and Schoen, 2021), with the evolution of ray flowers representing a special case of such changes—driven by the same genes but occurring only in some flowers within the inflorescence (Hileman, 2014). The high rate of reversals (losses) inferred for floral pseudocorollas in this study are concordant with the general pattern found for floral symmetry in angiosperms, whereby losses of zygomorphy are more likely to occur than gains when modeled with maximum-likelihood methods (Sauquet et al., 2017; Reyes et al., 2018). In the future, these important issues concerning evolvability of flower-like inflorescences may be properly addressed with hidden Markov models such as the precursor model (Marazzi et al., 2012; Tarasov, 2019).

Diversification of Apioideae

The phylogeny of Apioideae was shaped by extraordinarily numerous shifts in diversification rates, consistently exceeding 10 in all variants of trait-independent analyses and reaching

more than 30 for some runs of BAMM. Similar numbers have not been recorded in any other study of comparable phylogenetic scale (Baker and Couvreur, 2013; Reyes et al., 2015; Panero and Crozier, 2016; Xue et al., 2020) and are closer to the family-level analyses of all flowering plants with 30 shifts found by Magallón et al. (2019) and 27 by Tank et al. (2015). MEDUSA estimates in the mega-scale analysis of Smith and Brown (2018) recovered only 10 shifts in Apioideae.

Our understanding of ecological and morphological evolution in apioids (and Apiales in general) is full of gaps, and it remains difficult to reliably identify major drivers of their diversification. The explosive radiation of some clades identified in our study could have arisen from hybridization/introgression events (Panahi et al., 2015), long-distance dispersal (Sun et al., 2004; Chung et al., 2005) or expansion of gene families involved in the synthesis of biochemical compounds (Krieger et al., 2018), but none of these traits have been subject to detailed analyses. Although pseudanthia cannot explain diversification patterns observed in the entire subfamily (Table 2; Appendix S4C), they could have played an important role on a smaller scale, facilitating radiation of some large, panboreal genera such as *Heracleum*, the pseudocorollar representatives of which include many invasive, noxious weeds (Jahodová et al., 2007).

CONCLUSIONS

Our study indicates that flower-like inflorescences are scattered throughout the apioid phylogeny and are extremely labile evolutionarily, with recurrent gains and reversals occurring in most of the lineages that evolved this architecture. Like many other traits of Apioideae, pseudanthia may arise due to adaptive generalization and optimal use of local pollination niches. Furthermore, pseudocorollas can be used to mitigate trade-offs associated with the enlargement of floral display, especially under pollinator limitation. Surprisingly, the presence of pseudanthia cannot sufficiently explain the high variation in diversification rates recovered for Apioideae. The ecological importance of different pseudanthial architectures can be extrapolated from more general patterns, but without experimental studies on generalized pollination systems and reaching beyond “floricentrism” such hypotheses will remain highly speculative.

ACKNOWLEDGMENTS

We thank M. Chartier, Ł. Banasiak, and M. Zych for helpful discussions on methodological questions. We are also grateful to the Associate Editor J. Schönenberger and two anonymous reviewers for comments that improved this article.

AUTHOR CONTRIBUTIONS

J.B. with H.S. and K.S. developed ideas for the manuscript; J.B. gathered the data, performed analyses, and wrote the manuscript; H.S. and K.S. edited the manuscript.

DATA AVAILABILITY STATEMENT

All sequence alignments (before and after trimming) and maximum likelihood tree are available from TreeBase repository (www.treebase.org) under Study Accession URL: <http://purl.org/phylo/treebase/phyloids/study/TB2:S29132>.

ORCID

Jakub Baczyński  <https://orcid.org/0000-0001-5272-9053>

Hervé Sauquet  <https://orcid.org/0000-0001-8305-3236>

Krzysztof Spalik  <https://orcid.org/0000-0001-9603-6793>

REFERENCES

- Affolter, J. M. 1985. A monograph of the genus *Lilaeopsis* (Umbelliferae). *Systematic Botany Monographs* 6: 1–140.
- Ajani, Y., A. Ajani, J. M. Cordes, M. F. Watson, and S. R. Downie. 2008. Phylogenetic analysis of nrDNA ITS sequence reveals relationships within five groups of Iranian Apiaceae subfamily Apioideae. *Taxon* 57: 383–401.
- Alfaro, M. E., F. Santini, C. Brock, H. Alamillo, A. Dornburg, D. L. Rabosky, G. Carnevale, and L. J. Harmon. 2009. Nine exceptional radiations plus high turnover explain species diversity in jawed vertebrates. *Proceedings of the National Academy of Sciences, USA* 106: 13410–13414.
- Anderson, M. J., and D. C. I. Walsh. 2013. PERMANOVA, ANOSIM, and the Mantel test in the face of heterogeneous dispersions: what null hypothesis are you testing? *Ecological Monographs* 83: 557–574.
- Andersson, S. 1996. Floral display and pollination success in *Senecio jacobaea* (Asteraceae): interactive effects of head and corymb size. *American Journal of Botany* 83: 71–75.
- Andersson, S. 1999. The cost of floral attractants in *Achillea ptarmica* (Asteraceae): evidence from a ray removal experiment. *Plant Biology* 1: 569–572.
- Andersson, S. 2008. Pollinator and nonpollinator selection on ray morphology in *Leucanthemum vulgare* (oxeye daisy, Asteraceae). *American Journal of Botany* 95: 1072–1078.
- Baczyński, J., A. Miłobędzka, and Ł. Banasiak. 2021. Morphology of pollen in Apiales (asterids, eudicots). *Phytotaxa* 478: 1–32.
- Baker, W. J., and T. L. Couvreur. 2013. Global biogeography and diversification of palms sheds light on the evolution of tropical lineages. II. Diversification history and origin of regional assemblages. *Journal of Biogeography* 40: 286–298.
- Banasiak, Ł., M. Piwczynski, T. Uliński, S. R. Downie, M. F. Watson, B. Shakya, and K. Spalik. 2013. Dispersal patterns in space and time: a case study of Apiaceae subfamily Apioideae. *Journal of Biogeography* 40: 1324–1355.
- Banasiak, Ł., A. Wojewódzka, J. Baczyński, J.-P. Reduron, M. Piwczynski, R. Kurzyrna-Młynik, R. Gutaker, et al. 2016. Phylogeny of Apiaceae subtribe Daucinae and the taxonomic delineation of its genera. *Taxon* 65: 563–585.
- Beaulieu, J. M., and B. C. O'Meara. 2016. Detecting hidden diversification shifts in models of trait-dependent speciation and extinction. *Systematic Biology* 65: 583–601.
- Bell, C. R. 1971. Breeding systems and floral biology of the Umbelliferae; or, evidence for specialization in unspecialized flowers. In H. Heywood [ed.], *The Biology and Chemistry of the Umbelliferae*, 93–107. Academic Press, London, UK.
- Berger, B. A., V. Thompson, A. Lim, V. Ricigliano, and D. G. Howarth. 2016. Elaboration of bilateral symmetry across *Knautia macedonica* capitula related to changes in ventral petal expression of CYCLOIDEA-like genes. *EvoDevo* 7: 1.
- Björklund, M. 2019. Be careful with your principal components. *Evolution* 73: 2151–2158.
- Boyko, J. D., and J. M. Beaulieu. 2020. Generalized hidden Markov models for phylogenetic comparative datasets. *Methods in Ecology and Evolution* 12: 468–478.

- Brown, J. M., S. M. Hedtke, A. R. Lemmon, A., and E. M. Lemmon. 2010. When trees grow too long: investigating the causes of highly inaccurate Bayesian branch-length estimates. *Systematic Biology* 59: 145–161.
- Caetano, D. S., B. C. O'Meara, and J. M. Beaulieu. 2018. Hidden state models improve state-dependent diversification approaches, including biogeographical models. *Evolution* 72: 2308–2324.
- Calviño, C. L., and S. R. Downie. 2007. Circumscription and phylogeny of Apiaceae subfamily Saniculoideae based on chloroplast DNA sequences. *Molecular Phylogenetics and Evolution* 44: 175–191.
- Calviño, C. L., S. G. Martínez, and S. R. Downie. 2008. Morphology and biogeography of Apiaceae subfamily Saniculoideae as inferred by phylogenetic analysis of molecular data. *American Journal of Botany* 95: 196–214.
- Capella-Gutiérrez, S., J. M. Silla-Martínez, and T. Gabaldón. 2009. trimAl: a tool for automated alignment trimming in large-scale phylogenetic analyses. *Bioinformatics* 25: 1972–1973.
- Celedón-Neghme, C., W. L. Gonzáles, and E. Gianoli. 2007. Cost and benefits of attractive floral traits in the annual species *Madia sativa* (Asteraceae). *Evolutionary Ecology* 21: 247–257.
- Cerca, J., A. B. Agudo, S. Castro, A. Afonso, I. Alvarez, and R. Torices. 2019. Fitness benefits and costs of floral advertising traits: insights from rayed and rayless phenotypes of *Anacyclus* (Asteraceae). *American Journal of Botany* 106: 231–243.
- Chartier, M., S. Löfstrand, M. von Balthazar, S. Gerber, F. Jabbour, H. Sauquet, and J. Schönenberger. 2017. How (much) do flowers vary? Unbalanced disparity among flower functional modules and a mosaic pattern of morphospace occupation in the order Ericales. *Proceedings of the Royal Society, B, Biological Sciences* 284: 20170066.
- Chavent, M., V. Kuentz-Simonet, A. Labenne, and J. Saracco. 2014. Multivariate analysis of mixed data: the PCAmixdata R package preprint]. ArXiv:1411.4911, 132.
- Chen, C. H., and J. C. Wang 2001. Revision of the genus *Oreomyrrhis* Endl. (Apiaceae) in Taiwan. *Botanical Bulletin of Academia Sinica* 42: 303–312.
- Chung, K.-F., C.-I. Peng, S. R. Downie, K. Spalik, and B. A. Schaal. 2005. Molecular systematics of the trans-pacific alpine genus *Oreomyrrhis* (Apiaceae): phylogenetic affinities and biogeographic implications. *American Journal of Botany* 92: 2054–2071.
- Clarkson, J. J., A. R. Zuntini, O. Maurin, S. R. Downie, G. M. Plunkett, A. N. Nicolas, J. F. Smith, et al. 2021. A higher-level nuclear phylogenomic study of the carrot family (Apiaceae). *American Journal of Botany* 108: 1252–1269.
- Claßen-Bockhoff, R. 1990. Pattern analysis in pseudanthia. *Plant Systematics and Evolution* 171: 57–88.
- Claßen-Bockhoff, R., R. Ruonala, K. Bull-Hereñu, N. Marchant, and V. A. Albert. 2013. The unique pseudanthium of *Actinodium* (Myrtaceae)-morphological reinvestigation and possible regulation by CYCLOIDEA-like genes. *EvoDevo* 4: 8.
- Davila, Y. C., and G. M. Wardle. 2008. Variation in native pollinators in the absence of honeybees: implications for reproductive success of an Australian generalist-pollinated herb *Trachymene incisa* (Apiaceae). *Botanical Journal of the Linnean Society* 156: 479–490.
- Dilley, J. D., P. Wilson, and M. R. Mesler. 2000. The radiation of *Calochortus*: generalist flowers moving through a mosaic of potential pollinators. *Oikos* 89: 209–222.
- Downie, S. R., and D. S. Katz-Downie. 1996. A molecular phylogeny of Apiaceae subfamily Apioideae: evidence from nuclear ribosomal DNA internal transcribed spacer sequences. *American Journal of Botany* 83: 234–251.
- Downie, S. R., D. S. Katz-Downie, and K. J. Cho. 1996. Phylogenetic analysis of Apiaceae subfamily Apioideae using nucleotide sequences from the chloroplast *rpoCl* intron. *Molecular Phylogenetics and Evolution* 6: 1–18.
- Downie, S. R., K. Spalik, D. S. Katz-Downie, and J. P. Reduron. 2010. Major clades within Apiaceae subfamily Apioideae as inferred by phylogenetic analysis of nrDNA ITS sequences. *Plant Diversity and Evolution* 128: 111–136.
- Eisikowitch, D. 1980. The role of dark flowers in the pollination of certain Umbelliferae. *Journal of Natural History* 14: 737–742.
- Fambrini, M., and C. Pugliesi. 2017. CYCLOIDEA 2 clade genes: key players in the control of floral symmetry, inflorescence architecture, and reproductive organ development. *Plant Molecular Biology Reporter* 35: 20–36.
- Feng, C.-M., X. Liu, Y. Yu, D. Xie, R. G. Franks, and Q.-Y. (Jenny) Xiang. 2012. Evolution of bract development and B-class MADS box gene expression in petaloid bracts of *Cornus* s. l. (Cornaceae). *New Phytologist* 196: 631–643.
- Fernández-Mazuecos, M., J. L. Blanco-Pastor, A. Juan, P. Carnicero, A. Forrest, M. Alarcón, P. Vargas, and B. J. Glover. 2019. Macroevolutionary dynamics of nectar spurs, a key evolutionary innovation. *New Phytologist* 222: 1123–1138.
- FitzJohn, R. G. 2012. Diversitree: comparative phylogenetic analyses of diversification in R. *Methods in Ecology and Evolution* 3: 1084–1092.
- Francisco-Ortega, J., L. R. Goertzen, A. Santos-Guerra, A. Benabid, and R. K. Jansen. 1999. Molecular systematics of the *Asteriscus* alliance (Asteraceae: inuleae). I: evidence from the internal transcribed spacers of nuclear ribosomal DNA. *Systematic Botany* 24: 249–266.
- Gamisch, A. 2016. Notes on the statistical power of the binary state speciation and extinction (BISSE) model. *Evolutionary Bioinformatics* 12, EBO-S39732.
- Goldberg, E. E., S. P. Otto, J. C. Vamosi, I. Mayrose, N. Sabath, R. Ming, and T.-L. Ashman 2017. Macroevolutionary synthesis of flowering plant sexual systems. *Evolution* 71: 898–912.
- Gómez, J. M., A. J. Muñoz-Pajares, M. Abdelaziz, J. Lorite, and F. Perfectti. 2014. Evolution of pollination niches and floral divergence in the generalist plant *Erysimum mediohispanicum*. *Annals of Botany* 113: 237–249.
- Gómez, J. M., F. Perfectti, M. Abdelaziz, J. Lorite, A. J. Muñoz-Pajares, and J. Valverde. 2015. Evolution of pollination niches in a generalist plant clade. *New Phytologist* 205: 440–453.
- Goulson, D., K. Mcguire, E. E. Munro, S. Adamson, L. Colliar, K. J. Park, M. C. Tinsley, and A. S. Gilburn. 2009. Functional significance of the dark central floret of *Daucus carota* (Apiaceae) L.; Is it an insect mimic? *Plant Species Biology* 24: 77–82.
- Grindeland, J. M., N. Sletvold, and R. A. Ims. 2005. Effects of floral display size and plant density on pollinator visitation rate in a natural population of *Digitalis purpurea*. *Functional Ecology* 19: 383–390.
- Guo, X.-L., W. Gou, F.-M. Xie, S.-D. Zhou, and X.-J. He. 2020. *Hymenidium pilosum* (Apiaceae) is a synonym of *H. apiolens* based on morphology and molecular data. *Nordic Journal of Botany* 38. <https://doi.org/10.1111/njb.02864>
- Harder, L. D., and S. C. Barrett. 1995. Mating cost of large floral displays in hermaphrodite plants. *Nature* 373: 512–515.
- Harder, L. D., and S. D. Johnson. 2005. Adaptive plasticity of floral display size in animal-pollinated plants. *Proceedings of the Royal Society, B, Biological Sciences* 272: 2651–2657.
- Harder, L. D., C. Y. Jordan, W. E. Gross, and M. B. Routley. 2004. Beyond floriculture: the pollination function of inflorescences. *Plant Species Biology* 19: 137–148.
- Hileman, L. C. 2014. Trends in flower symmetry evolution revealed through phylogenetic and developmental genetic advances. *Philosophical Transactions of the Royal Society, B, Biological Sciences* 369: 20130348.
- Ishii, H. S., Y. Hirabayashi, and G. Kudo. 2008. Combined effects of inflorescence architecture, display size, plant density and empty flowers on bumble bee behaviour: experimental study with artificial inflorescences. *Oecologia* 156: 341–350.
- Jahodová, Š., S. Trybush, P. Pyšek, M. Wade, and A. Karp. 2007. Invasive species of *Heracleum* in Europe: an insight into genetic relationships and invasion history. *Diversity and Distributions* 13: 99–114.
- Jeffrey, C. 2009. Evolution of Compositae flowers. *Systematics, Evolution, and Biogeography of Compositae*, 131–138.

- Jiang, W., S.-Y. Chen, H. Wang, D.-Z. Li, and J. J. Wiens. 2014. Should genes with missing data be excluded from phylogenetic analyses? *Molecular Phylogenetics and Evolution* 80: 308–318.
- Joly, S., and D. J. Schoen. 2021. Repeated evolution of a reproductive polyphenism in plants is strongly associated with bilateral flower symmetry. *Current Biology* 31: 1515–1520.e3.
- Katinas, L., J. V. Crisci, R. S. Jabaily, C. Williams, J. Walker, B. Drew, J. M. Bonifacio, and K. J. Sytsma. 2008. Evolution of secondary heads in Nassauviinae (Asteraceae, Mutisiaeae). *American Journal of Botany* 95: 229–240.
- Katinas, L., and N. B. Forte. 2020. Capitulum compartmentalization in *Leucheria* (Nassauviaceae): insights into the evolution of Asteraceae inflorescence. *Taxon* 69: 679–693.
- Katoh, K., and D. M. Standley. 2013. MAFFT multiple sequence alignment software version 7: improvements in performance and usability. *Molecular Biology and Evolution* 30: 772–780.
- Katz-Downie, D. S., C. M. Valiejo-Roman, E. I. Terenteva, A. V. Troitsky, M. G. Pimenov, B. Lee, and S. R. Downie. 1999. Towards a molecular phylogeny of Apiaceae subfamily Apioideae: Additional information from nuclear ribosomal DNA ITS sequences. *Plant Systematics and Evolution* 216: 167–195.
- Kodandaramaiah, U., and G. Murali. 2018. What affects power to estimate speciation rate shifts? *PeerJ* 6: e5495.
- Koski, M. H. 2020. Macroevolution of flower color patterning: biased transition rates and correlated evolution with flower size. *Frontiers in Plant Science* 11: 945.
- Krieger, C., S. Roselli, S. Kellner-Thielmann, G. Galati, B. Schneider, J. Grosjean, A. Olry, et al. 2018. The CYP71AZ P450 subfamily: a driving factor for the diversification of coumarin biosynthesis in apiaceous plants. *Frontiers in Plant Science* 9.
- Lamborn, E., and J. Ollerton. 2000. Experimental assessment of the functional morphology of inflorescences of *Daucus carota* (Apiaceae): testing the “fly catcher effect”. *Functional Ecology* 14: 445–454.
- Lanfear, R., B. Calcott, S. Y. W. Ho, and S. Guindon. 2012. PartitionFinder: combined selection of partitioning schemes and substitution models for phylogenetic analyses. *Molecular Biology and Evolution* 29: 1695–1701.
- Lemmon, A. R., J. M. Brown, K. Stanger-Hall, and E. M. Lemmon. 2009. The effect of ambiguous data on phylogenetic estimates obtained by maximum likelihood and Bayesian inference. *Systematic Biology* 58: 130–145.
- Lindsey, A. H., and C. R. Bell. 1985. Reproductive biology of Apiaceae. II. Cryptic specialization and floral evolution in *Thaspium* and *Zizia*. *American Journal of Botany* 72: 231–247.
- Louca, S., and M. W. Pennell. 2020. Extant timetrees are consistent with a myriad of diversification histories. *Nature* 580: 502–505.
- Maddison, W. P., and R. G. FitzJohn. 2015. The unsolved challenge to phylogenetic correlation tests for categorical characters. *Systematic Biology* 64: 127–136.
- Magallón, S., L. L. Sánchez-Reyes, and S. L. Gómez-Acevedo. 2019. Thirty clues to the exceptional diversification of flowering plants. *Annals of Botany* 123: 491–503.
- Magee, A., C. Calvino, M. Liu, S. Downie, P. Tilney, and B. Wyk. 2010. New tribal delimitations for the early diverging lineages of Apiaceae subfamily Apioideae. *Taxon* 59: 567–580.
- Manchester, S. R., F. Grímsson, and R. Zetter. 2015. Assessing the fossil record of asterids in the context of our current phylogenetic framework. *Annals of the Missouri Botanical Garden* 100: 329.
- Marazzi, B., C. Ané, M. F. Simon, A. Delgado-Salinas, M. Luckow, and M. J. Sanderson. 2012. Locating evolutionary precursors on a phylogenetic tree. *Evolution* 66: 3918–3930.
- May, M. R., and B. R. Moore. 2016. How well can we detect lineage-specific diversification-rate shifts? A simulation study of sequential AIC methods. *Systematic Biology* 65: 1076–1084.
- Moore, B. R., S. Höhna, M. R. May, B. Rannala, and J. P. Huelsenbeck. 2016. Critically evaluating the theory and performance of Bayesian analysis of macroevolutionary mixtures. *Proceedings of the National Academy of Sciences, USA* 113: 9569–9574.
- Nakov, T., J. M. Beaulieu, and A. J. Alverson. 2019. Diatoms diversify and turn over faster in freshwater than marine environments. *Evolution* 73: 2497–2511.
- Nicolas, A. N., and G. M. Plunkett. 2014. Diversification times and biogeographic patterns in Apiales. *Botanical Review* 80: 30–58.
- Nielsen, L. R., M. Philipp, and H. R. Siegismund. 2002. Selective advantage of ray florets in *Scalesia affinis* and *S. pedunculata* (Asteraceae), two endemic species from the Galápagos. *Evolutionary Ecology* 16: 139–153.
- Niemirski, R., and M. Zych. 2011. Fly pollination of dichogamous *Angelica sylvestris* (Apiaceae): How (functionally) specialized can a (morphologically) generalized plant be? *Plant Systematics and Evolution* 294: 147–158.
- Nye, T. M. 2011. Principal components analysis in the space of phylogenetic trees. *Annals of Statistics* 39: 2716–2739.
- Ohara, M., and S. Higashi. 1994. Effects of inflorescence size on visits from pollinators and seed set of *Corydalis ambigua* (Papaveraceae). *Oecologia* 98: 25–30.
- Ohashi, K., A. Jürgens, and J. D. Thomson. 2021. Trade-off mitigation: a conceptual framework for understanding floral adaptation in multispecies interactions. *Biological Reviews* 96: 2258–2280.
- Ohashi, K., and T. Yahara. 1999. How long to stay on, and how often to visit a flowering plant? A model for foraging strategy when floral displays vary in size. *Oikos* 86: 386–392.
- Ohashi, K., and T. Yahara. 2001. Behavioural responses of pollinators to variation in floral display size and their influences on the evolution of floral traits. In L. Chittka and J. D. Thomson [eds.], *Cognitive ecology of pollination*, 274–296: Cambridge University Press, Cambridge.
- Ohashi, K., and T. Yahara. 2002. Visit larger displays but probe proportionally fewer flowers: counterintuitive behaviour of nectar-collecting bumble bees achieves an ideal free distribution. *Functional Ecology* 16: 492–503.
- Oksanen, J., F. G. Blanchet, R. Kindt, P. Legendre, P. R. Minchin, R. B. O’hara, G. L. Simpson, et al. 2013. Package ‘vegan’: community Ecology Package, version 2, 1–295. Website: <https://github.com/vegandevs/vegan>
- Panahi, M., Ł. Banasiak, M. Piwczyński, R. Puchalka, A. A. Oskolski, and K. Spalik. 2015. Phylogenetic relationships among *Dorema*, *Ferula* and *Leutea* (Apiaceae: Scandiceae: Ferulinae) inferred from nrDNA ITS and cpDNA noncoding sequences. *Taxon* 64: 770–783.
- Panero, J. L., and B. S. Crozier. 2016. Macroevolutionary dynamics in the early diversification of Asteraceae. *Molecular Phylogenetics and Evolution* 99: 116–132.
- Panero, J. L., S. E. Freire, L. Ariza Espinar, B. S. Crozier, G. E. Barboza, and J. J. Cantero. 2014. Resolution of deep nodes yields an improved backbone phylogeny and a new basal lineage to study early evolution of Asteraceae. *Molecular Phylogenetics and Evolution* 80: 43–53.
- Pérez-Bañón, C., T. Petanidou, and M. Á. Marcos-García. 2007. Pollination in small islands by occasional visitors: the case of *Daucus carota* subsp. *commutatus* (Apiaceae) in the Columbretes archipelago, Spain. *Plant Ecology* 192: 133–151.
- Plunkett, G. M., M. G. Pimenov, J. P. Reduron, E. V. Kljuykov, B. Y. Lee, B. E. van Wyk, P. M. Tilney, et al. 2018. Apiaceae. In K. Kubitzky [ed.], *The families and genera of vascular plants*. Springer, Cham.
- Polly, P. D., A. M. Lawing, A.-C. Fabre, and A. Goswami. 2013. Phylogenetic principal components analysis and geometric morphometrics. *Hystrix, the Italian Journal of Mammalogy* 24: 33–41.
- Polte, S., and K. Reinhold. 2013. The function of the wild carrot’s dark central floret: Attract, guide or deter? *Plant Species Biology* 28: 81–86.
- Rabosky, D. L. 2018. BAMM at the court of false equivalency: a response to Meyer and Wiens. *Evolution* 72: 2246–2256.
- Rabosky, D. L., and E. E. Goldberg. 2015. Model inadequacy and mistaken inferences of trait-dependent speciation. *Systematic Biology* 64: 340–355.

- Rabosky, D. L., M. Grundler, C. Anderson, P. Title, J. J. Shi, J. W. Brown, H. Huang, and J. G. Larson. 2014. BAMM tools: an R package for the analysis of evolutionary dynamics on phylogenetic trees. *Methods in Ecology and Evolution* 5: 701–707.
- Rabosky, D. L., J. S. Mitchell, and J. Chang. 2017. Is BAMM flawed? Theoretical and practical concerns in the analysis of multi-rate diversification models. *Systematic Biology* 66: 477–498.
- Ramírez-Barahona, S., H. Sauquet, and S. Magallón. 2020. The delayed and geographically heterogeneous diversification of flowering plant families. *Nature Ecology & Evolution* 4: 1232–1238.
- Reuther, K., and R. Claßen-Bockhoff. 2010. Diversity behind uniformity—Inflorescence architecture and flowering sequence in Apiaceae-Apioideae. *Plant Diversity and Evolution* 128: 181–220.
- Reyes, E., H. Morlon, and H. Sauquet. 2015. Presence in Mediterranean hotspots and floral symmetry affect speciation and extinction rates in Proteaceae. *New Phytologist* 207: 401–410.
- Reyes, E., S. Nadot, M. von Balthazar, J. Schönerberger, and H. Sauquet. 2018. Testing the impact of morphological rate heterogeneity on ancestral state reconstruction of five floral traits in angiosperms. *Scientific Reports* 8: 473.
- Reyes, E., H. Sauquet, and S. Nadot. 2016. Perianth symmetry changed at least 199 times in angiosperm evolution. *Taxon* 65: 945–964.
- Robertson, A. W. 1992. The relationship between floral display size, pollen carryover and geitonogamy in *Myosotis colensoi* (Kirk) Macbride (Boraginaceae). *Biological Journal of the Linnean Society* 46: 333–349.
- Ronse, A. C., Z. A. Popper, J. C. Preston, and M. F. Watson. 2010. Taxonomic revision of European *Apium*. L. s.l.: *Helosciadium* W. D. J. Koch restored. *Plant Systematics and Evolution* 287: 1–17.
- Roure, B., D. Baurain, and H. Philippe. 2013. Impact of missing data on phylogenies inferred from empirical phylogenomic data sets. *Molecular Biology and Evolution* 30: 197–214.
- Rudall, P. J. 2003. Monocot pseudanthia revisited: floral structure of the mycoheterotrophic family Triuridaceae. *International Journal of Plant Sciences* 164: S307–S320.
- Sanderson, M. J. 2002. Estimating absolute rates of molecular evolution and divergence times: a penalized likelihood approach. *Molecular Biology and Evolution* 19: 101–109.
- Sanz, M., R. Vilatersana, O. Hidalgo, N. Garcia-Jacas, A. Susanna, G. M. Schneeweiss, and J. Vallès. 2008. Molecular phylogeny and evolution of floral characters of *Artemisia* and allies (Anthemideae, Asteraceae): Evidence from nrDNA ETS and ITS sequences. *Taxon* 57: 66–78.
- Sauquet, H., M. von Balthazar, S. Magallón, J. A. Doyle, P. K. Endress, E. J. Bailes, E. B. de Morais, et al. 2017. The ancestral flower of angiosperms and its early diversification. *Nature Communications* 8: 16047.
- Sheppard, A. W. 1991. *Heracleum sphondylium* L. *Journal of Ecology* 79: 235–258.
- Simpson, A. G., P. J. Wagner, S. L. Wing, and C. B. Fenster. 2018. Binary-state speciation and extinction method is conditionally robust to realistic violations of its assumptions. *BMC Evolutionary Biology* 18: 69.
- Skeels, A., R. Dinnage, I. Medina, and M. Cardillo. 2021. Ecological interactions shape the evolution of flower color in communities across a temperate biodiversity hotspot. *Evolution Letters* 5: 277–289.
- Smith, S. A., and J. W. Brown. 2018. Constructing a broadly inclusive seed plant phylogeny. *American Journal of Botany* 105: 302–314.
- Smith, S. A., and B. C. O'Meara. 2012. treePL: divergence time estimation using penalized likelihood for large phylogenies. *Bioinformatics* 28: 2689–2690.
- Smith, S. D., and E. E. Goldberg. 2015. Tempo and mode of flower color evolution. *American Journal of Botany* 102: 1014–1025.
- Spalik, K., J. P. Reduron, and S. R. Downie. 2004. The phylogenetic position of *Peucedanum* sensu lato and allied genera and their placement in tribe Selineae (Apiaceae, subfamily Apioideae). *Plant Systematics and Evolution* 243: 189–210.
- Stamatakis, A. 2014. RAxML version 8: a tool for phylogenetic analysis and post-analysis of large phylogenies. *Bioinformatics* 30: 1312–1313.
- Stuessy, T. F., D. M. Spooner, and K. A. Evans. 1986. Adaptive significance of ray corollas in *Helianthus grosseserratus* (Compositae). *The American Midland Naturalist* 115: 191–197.
- Sun, F. J., S. R. Downie, and R. L. Hartman. 2004. An ITS-based phylogenetic analysis of the perennial, endemic Apiaceae subfamily Apioideae of western North America. *Systematic Botany* 29: 419–431.
- Sun, J.-F., Y.-B. Gong, S. S. Renner, and S.-Q. Huang. 2008. Multifunctional bracts in the dove tree *Davidia involucreta* (Nyssaceae: Cornales): rain protection and pollinator attraction. *American Naturalist* 171: 119–124.
- Tähtiharju, S., A. S. Rijpkema, A. Vetterli, V. A. Albert, T. H. Teeri, and P. Elomaa. 2012. Evolution and diversification of the *CYC/TB1* gene family in Asteraceae—a comparative study in *Gerbera* (Mutisieae) and sunflower (Heliantheae). *Molecular Biology and Evolution* 29: 1155–1166.
- Tank, D. C., J. M. Eastman, M. W. Pennell, P. S. Soltis, D. E. Soltis, C. E. Hinchliff, J. W. Brown, et al. 2015. Nested radiations and the pulse of angiosperm diversification: increased diversification rates often follow whole genome duplications. *New Phytologist* 207: 454–467.
- Tarasov, S. 2019. Integration of anatomy ontologies and evo-devo using structured Markov models suggests a new framework for modeling discrete phenotypic traits. *Systematic Biology* 68: 698–716.
- Thakur, S., B. Singh, N. Tashi, and H. Dutt. 2020. *Neconopodium paddarensis*, a new species of Apiaceae from Jammu and Kashmir, Western Himalaya, India. *Phytotaxa* 459: 285–290.
- Thomann, M., E. Imbert, R. C. Engstrand, and P.-O. Cheptou. 2015. Contemporary evolution of plant reproductive strategies under global change is revealed by stored seeds. *Journal of Evolutionary Biology* 28: 766–778.
- Thomson, J. D., and P. Wilson. 2008. Explaining evolutionary shifts between bee and hummingbird pollination: convergence, divergence, and directionality. *International Journal of Plant Sciences* 169: 23–38.
- Todzia, C. A. 1988. Chloranthaceae: *Hedyosmum*. *Flora Neotropica* 48: 1–138.
- Tucker, S. C. 1981. Inflorescence and floral development in *Houttuynia cordata* (Saururaceae). *American Journal of Botany* 68: 1017–1032.
- Valiejo-Roman, C. M., E. I. Terentieva, T. H. Samigullin, and M. G. Pimenov. 2002. Relationships among genera in Saniculoideae and selected Apioideae (Umbelliferae) inferred from nrITS sequences. *Taxon* 51: 91–101.
- Van Wyk, B. E., P. M. Tilney, and A. R. Magee. 2010. A revision of the genus *Glia* (Apiaceae, tribe Heteromorphae). *South African Journal of Botany* 76: 259–271.
- Vekemans, D., T. Viaene, P. Caris, and K. Geuten. 2012. Transference of function shapes organ identity in the dove tree inflorescence. *New Phytologist* 193: 216–228.
- Wen, J., Y. Yu, D.-F. Xie, C. Peng, Q. Liu, S.-D. Zhou, and X.-J. He. 2020. A transcriptome-based study on the phylogeny and evolution of the taxonomically controversial subfamily Apioideae (Apiaceae). *Annals of Botany* 125: 937–953.
- Westmoreland, D., and C. Muntan. 1996. The influence of dark central florets on insect attraction and fruit production in Queen Anne's lace (*Daucus carota* L.). *American Midland Naturalist* 135: 122–129.
- Wickham, H. 2016. ggplot2: elegant graphics for data analysis. Springer, New York.
- Wiens, J. J. 2003. Missing data, incomplete taxa, and phylogenetic accuracy. *Systematic Biology* 52: 528–538.
- Wiens, J. J. 2005. Can incomplete taxa rescue phylogenetic analyses from long-branch attraction? *Systematic Biology* 54: 731–742.
- Wiens, J. J., and M. C. Morrill. 2011. Missing data in phylogenetic analysis: reconciling results from simulations and empirical data. *Systematic Biology* 60: 719–731.
- Wiens, J. J., and J. Tiu. 2012. Highly incomplete taxa can rescue phylogenetic analyses from the negative impacts of limited taxon sampling. *PLoS One* 7: e42925.

- Wilson, P., and J. D. Thomson. 1996. How do flowers diverge? In D. C. Lloyd and C. H. B. Spencer [eds.], *Floral biology: studies on floral evolution in animal-pollinated plants*, 88–111. Springer, New York.
- Xue, B., X. Guo, J. B. Landis, M. Sun, C. C. Tang, P. S. Soltis, D. E. Soltis, and R. M. K. Saunders. 2020. Accelerated diversification correlated with functional traits shapes extant diversity of the early divergent angiosperm family Annonaceae. *Molecular Phylogenetics and Evolution* 142: 106659.
- Zhang, W., Q.-Y. (Jenny) Xiang, D. T. Thomas, B. M. Wiegmann, M. W. Frohlich, and D. E. Soltis. 2008. "Molecular evolution of *PISTILLATA*-like genes in the dogwood genus *Cornus* (Cornaceae)." *Molecular Phylogenetics and Evolution* 47: 175–195.
- Zhao, Y., S. K. Broholm, F. Wang, A. S. Rijpkema, T. Lan, V. A. Albert, T. H. Teeri, and P. Elomaa. 2020. TCP and MADS-box transcription factor networks regulate heteromorphic flower type identity in *Gerbera hybrida*. *Plant Physiology* 184: 1455–1468.
- Zhou, J., H. Peng, S. R. Downie, Z.-W. Liu, and X. Gong. 2008. A molecular phylogeny of Chinese Apiaceae subfamily Apioideae inferred from nuclear ribosomal DNA internal transcribed spacer sequences. *Taxon* 57: 402–416.
- Zych, M. 2002. Pollination biology of *Heracleum sphondylium* L. (Apiaceae): the advantages of being white and compact. *Acta Societatis Botanicorum Poloniae* 71: 163–170.
- Zych, M. 2007. On flower visitors and true pollinators: the case of protandrous *Heracleum sphondylium* L. (Apiaceae). *Plant Systematics and Evolution* 263: 159–179.
- Zych, M., R. R. Junker, M. Nepi, M. Stpiczyńska, B. Stolarska, and K. Roguz . 2019. Spatiotemporal variation in the pollination systems of a supergeneralist plant: Is *Angelica sylvestris* (Apiaceae) locally adapted to its most effective pollinators? *Annals of Botany* 123: 415–428.
- Zych, M., B. Michalska, and E. Krasicka-Korczyńska. 2014. Myophily in the critically endangered umbelliferous plant *Ostericum palustre* Besser (Apiaceae). *Plant Systematics and Evolution* 300: 187–196.

SUPPORTING INFORMATION

Additional supporting information may be found in the online version of the article at the publisher's website.

Appendix S1. List of accessions for molecular markers used in phylogenetic reconstruction.

Appendix S2. Morphological data set with a complete list of references.

Appendix S3. Information about fossils used for phylogeny calibration with age and node justifications and references.

Appendix S4. Graphs illustrating transition rate matrices (A, B) used in corHMM and trait-dependent diversification analyses with pseudocorollas encoded as a single state and results of the model-fitting (C) and stochastic mapping (D) conducted for this variant of analyses.

Appendix S5. Graphs with transition rate matrices used in corHMM (A) and trait-dependent diversification analyses (B) and marginal likelihood ancestral character estimation conducted separately for types of pseudocorollas (C) and size (D).

Appendix S6. Results of the betadisper (A) and NMDS (B) analyses.

Appendix S7. Four Excel sheets containing information about species richness provided for MEDUSA (A) or BAMM (B), calculations of sampling fraction for trait-dependent analyses (C), and data on apioid biodiversity according to Plants of the World Online database (POWO) (D).

Appendix S8. Phylogenetic tree of apioids with mapped bootstrap/SH-aLRT support. All major clades/tribes are collapsed into triangles.

Appendix S9. Plots of all possible two-dimensional combinations for the first five principal components.

Appendix S10. Phylorate plots for all variants of MEDUSA (A–F) and BAMM (G–X) analyses.

How to cite this article: Baczyński, J., H. Sauquet, and K. Spalik. 2022. Exceptional evolutionary lability of flower-like inflorescences (pseudanthia) in Apiaceae subfamily Apioideae. *American Journal of Botany* 109(3): 437–455.
<https://doi.org/10.1002/ajb2.1819>